Journal of Engineering and Applied Sciences 13 (6): 1414-1420, 2018
ISSN: 1816-949X

In Vitro Antiproliferative Effect, Cytotoxicity and Apoptosis Study of Biogenic Silver Nanoparticles Synthesized Using *Sterculia quadrifida* leaf Extract

Vishnu Rajendran
Department of Physics, Bishop Moore College, Mavelikara, Kerala, India

Abstract: Bio-nano synthesis and its widespread applications have become essential for sustainable development and welfare of humanity. The present study reports a biosynthetic pathway to produce highly stable, bio-inspired silver Nanoparticles (AgNPs) using fresh *Sterculia quadrifida* leaves. Following the traditional approach, UV-visible spectroscopy confirmed the formation of AgNPs. AFM and TEM results revealed their size, morphology and crystalline nature. Moreover, FTIR analysis exposed the nature of biomolecules adhering to the surface of silver nanoparticles which increased their stability. *Sterculia quadrifida* extracts rendered excellent reducing capability. Consequently, this procedure proved to be simpler, eco-friendly, cost-effective, reproducible and compatible with medical and pharmaceutical applications as well as large-scale commercial production. The nanoparticles, thus, synthesized, exhibited effective antimicrobial activity and AgNPs together with phytochemicals resulted in a strong antiproliferative effect. As such MTT assay helped to determine the levels of cytotoxicity. Furthermore, the study of apoptosis elucidated the possibility of employing AgNPs for programmed cell death. Since, increased apoptosis is a characteristic feature of AIDS, Alzheimer's and Parkinson's disease and decreased apoptosis trigger lupus or cancer, AgNPs can induce apoptosis in such cancer or tumor cells.

Key words: *Sterculia quadrifida*, AgNPs, UV-vis-spectroscopy, AFM, TEM, antiproliferative, cytotoxicity

INTRODUCTION

Today, we have entered the realms of nano dimension where science has paved way for creation and manipulation of ultra-small structures or materials at atomic, molecular and macromolecular scales giving birth to properties differing much from those at a larger scale (Gleiter, 2009). As such, nanoscience and nanotechnology has revolutionized the present era and helped humanity to make a giant leap into the future. Among various noble metal nanoparticles, silver nanoparticles have gained utmost importance due to their size, distribution and morphology (Cao, 2004). Precise control over these attributes helps to decide the physical properties of silver nanoparticles including the Surface Plasmon Resonance (SPR). Colloidal silver also exhibits strong antimicrobial and anticancer activities. Even though, there are several ways to synthesize silver nanoparticles such as laser ablation, electron irradiation, gamma irradiation, microwave processing, chemical reduction, photo-induced chemical methods, etc., most of them use high amounts of energy and hazardous chemicals which often result in AgNPs having extreme toxicity along with unnecessary substituents attached to them. However, we can overcome these limitations and technical hitches by employing biological methods, incorporated with green chemistry routes which result in an eco-friendly synthesis process (Mansoori, 2005). Biomolecules like proteins, phenols and flavonoids present in plants play a pivotal role to reduce ordinary silver into nanoparticles. Thus, the result is an eco-friendly method which is simple, cost-effective, facile and reproducible.

The present article reports a similar biosynthetic pathway to create highly stable, bio-inspired Silver Nanoparticles (AgNPs) using fresh *Sterculia quadrifida* leaves (Bayazit, 2010). *Sterculia quadrifida*, a medicinal plant having high phenol content is rich in secondary metabolites. Its leaves can calm sore eyes and have attained immense popularity due to its antibacterial and antioxidant activities. So far, there have been no reports on the synthesis of nanoparticles by using its leaf extract. The biosynthesized AgNPs exhibited excellent antibacterial, anticancer and antitumor activity.

MATERIALS AND METHODS

Material collection: Silver Nitrate ($AgNO_3$) of AR grade ($\geq$99.5% purity), Acridine Orange (AO) and Ethidium Bromide (EB) were purchased from Sigma-Aldrich, India. All glassware was cleaned with aqua regia and rinsed several times with deionized water. The fresh young leaves of *Sterculia quadrifida* were collected locally

in the month of April 2016. Four pathogenic bacterial strains-Staphylococcus, *Salmonella typhi*, *Escherichia coli* and Pseudomonas were procured from the microbial type culture collection (MTCC, Chandigarh, India). L929 (fibroblast) and SW480 (Colon carcinoma) cell lines were procured from National Centre for Cell Sciences (NCCS), Pune, India.

Preparation of the leaf extract: Fresh leaves of *Sterculia quadrifida* were collected locally and 50 g of these leaves were washed initially with tap water. Then, they were washed with deionized water several times to remove all impurities. Next, the dirt free leaves were chopped into fine pieces and taken into a 1000 mL beaker containing 250 mL deionized water. Next, it was boiled at 373 K for 15 min. Finally, the raw extract obtained was filtered twice with Whatman cellulose filter paper grade 42:2.5 μm and the filtered extract was used for further reduction of Ag^+ to Ag^0.

Phytochemical analysis of *Sterculia quadrifida* leaf extract: Analysis of the leaf extract was carried out to detect the presence of phytochemical constituents such as alkaloids, flavonoids, phenols, saponins, tannins, steroids, glycosides, etc.

Synthesis of silver nanoparticle: A freshly prepared aqueous solution of 1 mm $AgNO_3$ was used for the synthesis of AgNPs. The 1.0 mL of aqueous leaf extract was added to 10 mL of $AgNO_3$ solution and was stirred for 10 min at room temperature (sample A1). The appearance of a yellowish brown color within 8-10 min indicated the formation of nanoparticles. Similarly, samples A2-A5 were synthesized by adding 1.5, 2.0, 2.5 and 3.0 mL extracts, respectively.

Characterization of green synthesized silver nanoparticles

Visual examination: The color of the leaf extract was noted prior to the synthesis of AgNPs. A visible color change (yellow-reddish brown) during the experiment verifies the formation of biogenic-AgNPs (Krishnaraj *et al*., 2010).

UV-visible spectra analysis: Leaving behind a long legacy of nano-dimensional analysis, UV-visible absorption spectroscopy helps to characterize the nanoparticles, thereby shedding light on their optical properties and electronic structure. It is generally used to confirm the formation and stability of metal nanoparticles in aqueous solution (Krishnaraj *et al*., 2010; Mittal *et al*., 2015). JASCO UV-visible spectrophotometer (Model: V-650) having an optical wavelength of 10 mm and a resolution of 0.1 nm verified the formation of AgNPs. Baseline correction employing deionized water and UV-visible spectral analysis was performed for all samples within the wavelength range of 300-550 nm.

Atomic Force Microscope (AFM) analysis: A small volume of the synthesized AgNPs was spread on a well-cleaned glass slide and was dried using a current of nitrogen at room temperature. It was then mounted on the stub of a Correlative Raman-AFM α 300 RA microscope which is often employed for high-resolution nanoscale surface characterization. Images were obtained in AC mode (tapping mode) with a depth resolution <0.3 nm and lateral resolution ~1 nm. It employed a green laser source (532 nm) with 0.3 nm Raman spot size and 25, 50 and 100 μm pinhole size.

Transmission Electron Microscopy (TEM) analysis: TEM provides us with the shape and crystal structure (if any) as well as the size of the particles in the bulk. Test samples were prepared using 109 coatings of aqueous AgNP drops on carbon-coated copper grids which were kept aside for 5 min and the extra solution was removed using blotting paper. Then, the grid was exposed to Infra Red (IR) light for drying. The grid containing silver nanoparticles was scanned using Transmission Electron Microscope (Mittal *et al*., 2015). Consequently, the TEM images were obtained using a Jeol/JEM 2100 LaB6 instrument operated at 200 kV. It had a resolution of 0.23 nm for point and 0.14 nm for lattice analysis.

Fourier Transforms Infra-Red (FT-IR) spectroscopy analysis: Centrifugation of the biosynthesized AgNPs solution at 5,000 rpm for 30 min yielded nanoparticles, free of any kind of biomass residue or adhering compounds. Together with redispersion in 10 mL sterile distilled water, repeated centrifugation resulted in a purified suspension. In the same fashion, repetition of a series of redispersion and centrifugation processes yielded a high pure suspension. Finally, freeze-drying of the suspension provided us with a dried powder which was further analyzed using a Bruker Optik GmbH Tensor 27 FT-IR Spectrometer (Huth *et al*., 2012; Berthomieu and Hienerwadel, 2009).

Antimicrobial studies: From ancient times, humanity greatly reveres silver and its salts for exhibiting strong antimicrobial activity. We also analyzed our biosynthesized AgNPs for the same. Four bacterial strains were employed to study the antibacterial properties. Three gram-negative strains *Escherichia coli* MTCC 585,

Pseudomonas, Salmonella typhi and a gram-positive strain Staphylococcus were used in our study. These bacterial strains were streaked on nutrient agar and single pure culture was streaked on nutrient agar slants and stored at 4°C to keep the strains viable (Gavhane *et al*., 2012; Arokiyaraj *et al*., 2014).

Determination of *in vitro* antiproliferative effect of biosynthesized AgNPs on cultured SW480 cell line: SW480 (Colon carcinoma) cell line, cultured using DMEM (Dulbecco's Modified Eagle's Medium) supplemented with 10% FBS, L-glutamine, Sodium bicarbonate and an antibiotic solution containing Penicillin (100 U/mL), Streptomycin (100 μg/mL) and Amphotericin B (2.5 μg/mL) in 25 cm^2 tissue culture flask were kept in a humidified 5% CO_2 incubator-NBS (New Brunswick Shakers, Eppendorf, Germany) at 37°C. Inverted Phase Contrast Microscopy (Olympus CKX41 with Optika Pro5 CCD camera), followed by an MTT assay provided the results regarding cell viability (Gerlier and Thomasset, 1986). Microplate reader operated at 570 nm provided the absorbance values (Lorenzen and Kennedy, 1993; Valadez-Vega *et al*., 2011). The percentage of growth inhibition was calculated using Eq. 1:

$$\text{Percentage viability (\%)} = \text{Mean OD of samples} \times (\text{Mean OD of control group})^{-1} \times 100$$

The cytotoxic effect of biosynthesized AgNPs on cultured L929 cells: L929 (fibroblast) cell line was also cultured using DMEM supplemented with 10% FBS, L-glutamine, Sodium bicarbonate and an antibiotic solution containing Penicillin (100 U/mL), Streptomycin (100 μg/mL) and Amphotericin B (2.5 μg/mL) in a 25 cm^2 tissue culture flask. An NBS shaker incubator having humidified 5% CO_2 kept the cultured cell lines incubated at 37°C. Inverted phase contrast microscopy and MTT assay provided the percentage viability of cells. An appreciable change in the morphology or constitution of the cells pointed towards cytotoxicity (Lewinski *et al*., 2008; Martinez-Gutierrez *et al*., 2010).

Determination of apoptosis by Acridine Orange (AO) and Ethidium Bromide (EB) double staining: Morphological detection of apoptotic and necrotic cells was carried out using DNA-binding dyes AO and EB (Darzynkiewicz *et al*., 1992; Ribble *et al*., 2005; Liu *et al*., 2015). After treatment with different concentrations of AgNPs, the cells were washed with cold Phosphate-Buffered Saline (PBS) and then stained with a mixture of AO (100 μg/mL) and EB (100 μg/mL) at room temperature for 10 min. Then, 1×PBS was used twice to wash the stained cells. Later, they were observed under the blue filter (excitation) of a fluorescent microscope (Olympus CKX41 with an Optika Pro5 camera) (Darzynkiewicz *et al*., 1992; Zhang *et al*., 1998).

RESULTS AND DISCUSSION

Qualitative analysis and visual examination: Phytochemical analysis of the leaf extract revealed the presence of several organic groups capable of imparting strong reducing properties (Shihabudeen *et al*., 2010). The major plant chemicals that were present are given in Table 1.

The leaf extract had a pale yellow color and appeared turbid soon after adding $AgNO_3$. Meanwhile, the intensity of the color increased gradually from pale yellow to dark brown with the passage of time and finally attained reddish brown color at the end of the experiment (Fig. 1).

Evidently, the change in color occurs due to Surface Plasmon Resonance (SPR) which is the collective oscillation of all the "free" electrons within the conduction band of nanoparticles while being excited with light at particular wavelengths. Therefore, the formation of AgNPs can be confirmed. Also, the red shift with the passage of time can be attributed to increased agglomeration. There is no significant change beyond 240 min, thereby indicating the completion of the reduction reaction.

UV-visible spectral analysis: Silver nanoparticles generally exhibit a UV-visible absorption peak in the range 400-500 nm. The formation of AgNPs was initially

Table 1: Qualitative analysis of *Sterculia quadrifida* leaf extract

Phytochemicals	Water extract	Phytochemicals	Water extract
Alkaloids	Absent	Phenols	Present
Carbohydrates	Present	Saponins	Present
Glycosides	Absent	Tannins	Present
Steroids	Absent	Amino acids	Present
lavonoids	Present	Fatty acids	Present

Fig. 1: Biosynthesized silver nanoparticles

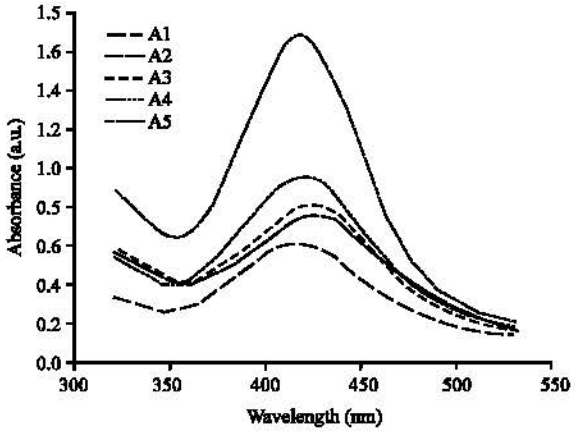

Fig. 2: UV-visible absorption spectra of biosynthesized AgNP

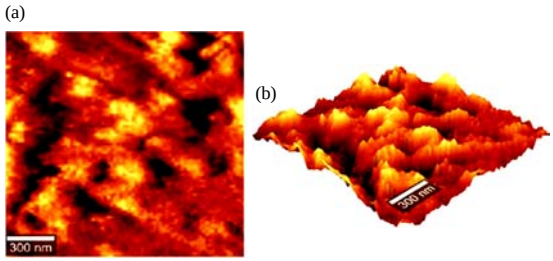

Fig. 3: AFM image showing AgNPs

confirmed using UV-visible spectroscopy (Fig. 2) which is attributed to the phenomenon of "SPR" (Smitha *et al*., 2008; Amendola *et al*., 2010). As such, SPR determines the polarizability of the metal and is responsible for shifting resonance to optical frequencies. The SPR band of sample A1 appears at 434 nm with a low intensity. The SPR band of A2-A5 samples appears at 423, 425, 423, 419 nm respectively. Additionally, increase in the volume of extract induces an equivalent increase in the absorption maximum. The broad SPR at lower volumes of extract is due to the formation of anisotropic particles whereas a larger quantity ensures a narrow and symmetric SPR band (Philip, 2010).

AFM analysis: AFM analysis is often employed to understand the morphology of biosynthesized AgNPs (Fig. 3). AFM image confirms the spherical shape of the particles and again the tendency for the particles to aggregate. The average size of particles was found to be 15-20 nm. The clumping of nanoparticles is essentially due to the presence of bio-molecules adhering to the surface of nanoparticles. Repeated centrifugation or ultracentrifugation, followed by redispersion in deionized water can reduce the rate of agglomeration (Shahoon,

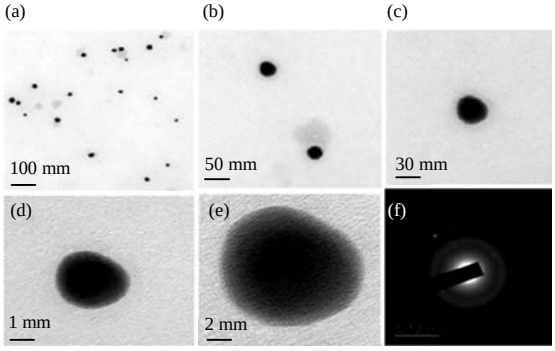

Fig. 4: TEM image showing AgNPs under various resolutions

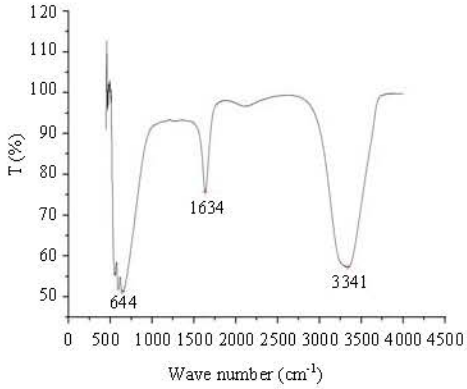

Fig. 5: FTIR spectra of bio-nano silver

2013). Furthermore, ultrasonication combined with the addition of a stabilizing agent such as Polyvinyl Alcohol (PVA) can yield good stability.

TEM analysis: Transmission Electron Microscopy offers one of the highest resolutions that we can achieve. This method helps us to observe the particle size of a material in nano-dimension and study the crystal structure meticulously (Rao *et al*., 2010). The TEM images of AgNPs synthesized at room temperature (25°C) were obtained (Fig. 4 and 5). The size distribution of AgNPs elucidated that they were narrow and mostly in the range of 5-25 nm with some of them having diameters close to 50 nm. Also, the extract proved to be an effective stabilizing agent by reducing agglomeration.

FT-IR analysis: FT-IR spectroscopy measurements were carried out to identify the biomolecules adhering specifically on the metal surface and the local molecular environment of capping agent associated with the nanoparticles.

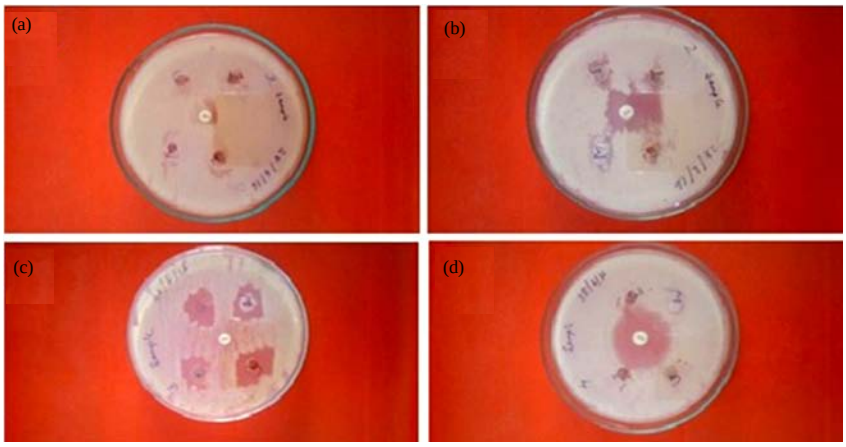

Fig. 6: Antimicrobial activities of AgNPs against: a) Staphylococcus; b) *Salmonalla typhi*; c) *Escherichia coli* and d) Pseudomon as respectively

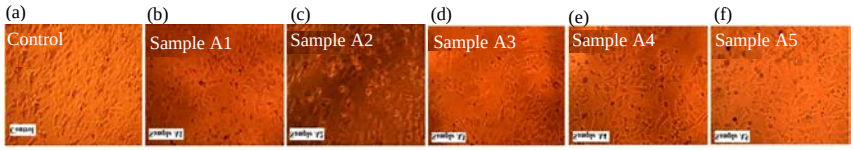

Fig. 7: The antiproliferative effect of biosynthesized AgNPs; a-f): Control, Sample A1-A5

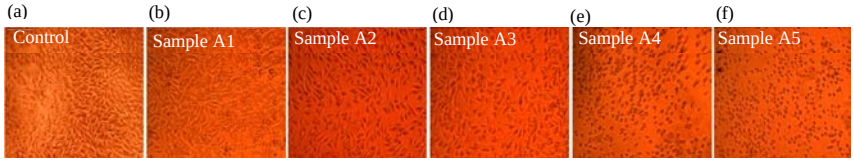

Fig. 8: The cytotoxic effect of biosynthesized AgNPs; a-f): Control, Sample A1-A5

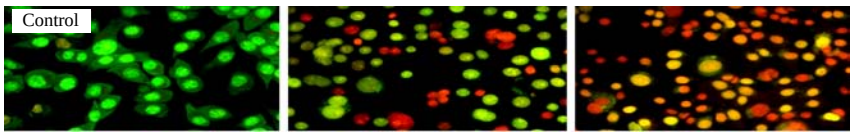

Fig. 9: Apoptosis results using AO and EB dyes

Figure 5 shows a broad peak in higher energy region 3341 cm^{-1} which characterizes the polysaccharides from the extract. This absorption frequency is assigned to the OeH group. The absorption band observed at 1634 cm^{-1} can be assigned to the amide (- $CONH_2$) groups of protein or to the carbonyl (C = O) stretching vibration group. The prominent band at 644 cm^{-1} is assigned to the aromatic class. These organic groups form a protective layer around the metal nanoparticles to prevent agglomeration and increase their stability.

Antimicrobial studies: Both gram-positive and gram-negative bacteria were inhibited by the AgNPs solution. Moreover, the inhibitory nature of these solutions increased with the amount of extract involved in the preparation of AgNPs (Fig. 6-9) (Martinez-Gutierrez *et al*., 2010). The size of inhibition zones indicates the relative extent of antimicrobial activity of AgNPs (Table 2). The antimicrobial activity of AgNPs can be associated with the fact that silver ions delivered by the nanoparticles promoted lysis in bacteria and

Table 2: Antibacterial activity of biosynthesized AgNPs

	Zone inhibition (cm)			
Microorganisms	Sample 1	Sample 2	Sample 3	Penicillin
Staphylococcus	2.0	2.1	2.0	1.5
Salmonalla typhi	1.3	1.1	1.5	2.0
Escherichia coli	1.5	1.6	1.7	1.5
Pseudomonas	1.1	1.3	1.5	2.3

Table 3: The antiproliferative effect of biosynthesized AgNPs

Samples	Average OD at 540 nm	Percentage viability
Control	0.6132	100.00000
A1 (1.0 µL extract+10 µL $AgNO_3$)	0.5584	68.58792
A2 (1.5 µL extract+10 µL $AgNO_3$)	0.5028	63.38972
A3 (2.0 µL extract+10 µL $AgNO_3$)	0.4906	57.07799
A4 (2.5 µL extract+10 µL $AgNO_3$)	0.4045	55.69304
A5 (3.0 µL extract+10 µL $AgNO_3$)	0.3331	45.86219

Table 4: The cytotoxic effect of biosynthesized AgNPs

Samples	Average OD at 540 nm	Percentage viability
Control	0.8897	100.00000
A1 (1.0 µL extract+10 µL $AgNO_3$)	0.8176	91.89614
A2 (1.5 µL extract+10 µL $AgNO_3$)	0.7294	81.98269
A3 (2.0 µL extract+10 µL $AgNO_3$)	0.6921	77.79027
A4 (2.5 µL extract+10 µL $AgNO_3$)	0.5440	61.14421
A5 (3.0 µL extract+10 µL $AgNO_3$)	0.4896	55.02979

ultimately led to a cellular breakdown and cell death. Hence, biogenic-AgNPs will prove beneficial for medical applications, industrial processing and enhancement of personal health care facilities.

Determination of *in vitro* antiproliferative effect by MTT assay: Rounding and shrinking of cells could be observed in samples A1-A3. Granulation and vacuolization in the cytoplasm of the cells were prominent in samples A4 and A5. These features clearly indicated the cytotoxic effect of AgNPs. Next, the percentage of growth inhibition was calculated and tabulated for each sample (Table 3). The antiproliferative effect of biosynthesized AgNPs (Table 3) (Shahoon, 2013).

The cytotoxic effect of biosynthesized AgNPs: Cytotoxicity is defined as the quality of being toxic to cells. The ability of cytotoxic agents to kill or damage cells which are reproducing rapidly determines their effectiveness against cancer or tumor cells (Valadez-Vega *et al*., 2011; Guo *et al*., 2014). The viability measurements using inverted phase contrast microscopy clearly depicted the cytotoxic nature of AgNPs. It was followed by MTT assay for assessing the cell metabolism and the obtained values were tabulated (Table 4).

Undoubtedly, the observed results strongly profile that there was a concentration dependent cytotoxic effect of biosynthesized AgNPs (Jeyaraj *et al*., 2013). As such, SW480 cells treated with AgNPs showed a steady decrease in viability.

Apoptosis results using Acridine Orange (AO) and Ethidium Bromide (EB): AO was taken up by both viable and non-viable cells and emitted green fluorescence if intercalated into double stranded nucleic acid (DNA). On the other hand, EB was taken up only by non-viable cells and emits red fluorescence by intercalation into DNA (Riccardi and Nicoletti, 2006). Hence, the cells were divided into four categories as follows:

- Living cells (normal green nucleus)
- Early apoptotic (bright green nucleus with condensed or fragmented chromatin)
- Late apoptotic (orange-stained nuclei with chromatin condensation or fragmentation)
- Necrotic cells (uniformly orange-stained cell nuclei

From the images, it is evident that biogenic-AgNPs were able to increase the amount of apoptosis with limited amount of necrosis. As such, we can employ these AgNPs as a viable alternative for tackling diseases such as cancer, tumor, etc.

CONCLUSION

The current research eports a bio-synthetic pathway for production of silver nanoparticles using *Sterculia quadrifida* leaf extract. The extract enacted the roles of reductant, size controller and stabilizing agent at room temperature, thereby providing us with a rapid yield of biogenic nanoparticles. Moreover, the rate of formation of AgNPs depended primarily on the amount of extract employed. Also, the obtained nanoparticles were capable of rendering significant antibacterial efficacy. As such, the presence of phytochemicals, cytotoxicity and antiproliferative activity indicate that AgNPs have widespread applications in the biomedical field. In addition to this, increased rate of apoptosis indicates that they can effectively tackle diseases such as cancer, tumor, lupus, etc. Accordingly, we can also achieve efficient drugdelivery using AgNPs in conjugation with peptides which needs further research and development. Finally, this procedure proved to have several advantages such as simplicity, eco-friendliness, cost-effectiveness, reproducibility and compatibility with various bio-physical, medical and pharmaceutical applications.

REFERENCES

Amendola, V., O.M. Bakr and F. Stellacci, 2010. A study of the surface plasmon resonance of silver nanoparticles by the discrete dipole approximation method: Effect of shape, size, structure and assembly. Plasmonics, 5: 85-97.

Arokiyaraj, S., M.V. Arasu, S. Vincent, N.U. Prakash and S.H. Choi *et al*., 2014. Rapid green synthesis of silver nanoparticles from Chrysanthemum indicum L. and its antibacterial and cytotoxic effects: An in vitro study. Intl. J. Nanomed., 9: 379-388.

Bayazit, V.A.H.D.E.T.T.I.N., 2010. Biological activities of nanomaterials (bufadienolides, peptides and alkoloids) in the skin of amphibian on Gammarus pulex L. Digest J. Nanomater. Biostructures, 5: 347-354.

Berthomieu, C. and R. Hienerwadel, 2009. Fourier Transform Infrared (FTIR) spectroscopy. Photosynth. Res., 101: 157-170.

Cao, G., 2004. Nanostructures and Nanomaterials: Synthesis, Properties and Applications. 1st Edn., Imperial College Press, London, ISBN-13: 978-1860944802, Pages: 433.

Darzynkiewicz, Z., S. Bruno, G. Del Bino, W. Gorczyca, M.A. Hotz, P. Lassota and F. Traganos, 1992. Features of apoptotic cells measured by flow cytometry. Cytometry, 13: 795-808.

Gavhane, A.J., P. Padmanabhan, S.P. Kamble and S.N. Jangle, 2012. Synthesis of silver nanoparticles using extract of neem leaf and Triphala and evaluation of their antimicrobial activities. Int. J. Pharma Bio Sci., 3: 88-100.

Gerlier, D. and N. Thomasset, 1986. Use of MTT colorimetric assay to measure cell activation. J. Immunol. Methods, 94: 57-63.

Gleiter, H., 2009. Nanoscience and nanotechnology: The key to new studies in areas of science outside of nanoscience and nanotechnology. MRS. Bull., 34: 456-464.

Guo, D., Y. Zhao, Y. Zhang, Q. Wang and Z. Huang *et al*., 2014. The cellular uptake and cytotoxic effect of silver nanoparticles on chronic myeloid leukemia cells. J. Biomed. Nanotechnol., 10: 669-678.

Huth, F., A. Govyadinov, S. Amarie, W. Nuansing and F. Keilmann *et al*., 2012. Nano-FTIR absorption spectroscopy of molecular fingerprints at 20 nm spatial resolution. Nano Lett., 12: 3973-3978.

Jeyaraj, M., G. Sathishkumar, G. Sivanandhan, D. MubarakAli and M. Rajesh *et al*., 2013. Biogenic silver nanoparticles for cancer treatment: An experimental report. Colloids Surfaces B: Biointerfaces, 106: 86-92.

Kent, R.D. and P.J. Vikesland, 2012. Controlled evaluation of silver nanoparticle dissolution using atomic force microscopy. Environ. Sci. Technol., 46: 6977-6984.

Krishnaraj, C., E.G. Jagan, S. Rajasekar, P. Selvakumar and P.T. Kalaichelvan *et al*., 2010. Synthesis of silver nanoparticles using Acalypha indica leaf extracts and its antibacterial activity against water borne pathogens. Colloids Surf. B. Biointerfaces, 76: 50-56.

Lewinski, N., V. Colvin and R. Drezek, 2008. Cytotoxicity of nanoparticles. Small, 4: 26-49.

Liu, K., P.C. Liu, R. Liu and X. Wu, 2015. Dual AO/EB staining to detect apoptosis in osteosarcoma cells compared with flow cytometry. Med. Sci. Monit. Basic Res., 21: 15-20.

Lorenzen, A. and S.W. Kennedy, 1993. A fluorescence-based protein assay for use with a microplate reader. Anal. Biochem., 214: 346-348.

Mansoori, G.A., 2005. Principles of Nanotechnology: Molecular-Based Study of Condensed Matter in Small Systems. World Scientific Publishing Co Inc., New Jersey, USA., ISBN: 981-256-154-4, Pages: 335.

Martinez-Gutierrez, F., P.L. Olive, A. Banuelos, E. Orrantia and N. Nino *et al*., 2010. Synthesis, characterization and evaluation of antimicrobial and cytotoxic effect of silver and titanium nanoparticles. Nanomed.: Nanotechnol. Biol. Med., 6: 681-688.

Mittal, A.K., D. Tripathy, A. Choudhary, P.K. Aili and A. Chatterjee *et al*., 2015. Bio-synthesis of silver nanoparticles using Potentilla fulgens wall ex hook and its therapeutic evaluation as anticancer and antimicrobial agent. Mater. Sci. Eng. C., 53: 120-127.

Philip, D., 2010. Green synthesis of gold and silver nanoparticles using Hibiscus rosa sinensis. Physica E. Low Dimensional Syst. Nanostructures, 42: 1417-1424.

Rao, D.S., K. Muraleedharan and C.J. Humphreys, 2010. TEM specimen preparation techniques. Microsc. Sci. Technol. Appl. Educ., 2010: 1232-1244.

Ribble, D., N.B. Goldstein, D.A. Norris and Y.G. Shellman, 2005. A simple technique for quantifying apoptosis in 96-well plates. BMC. Biotechnol., 5: 1-12.

Riccardi, C. and I. Nicoletti, 2006. Analysis of apoptosis by propidium iodide staining and flow cytometry. Nat. Protocols, 1: 1458-1461.

Shahoon, H., 2013. The comparison of silver and hydroxyapatite nanoparticles biocompatibility on l929 fibroblast cells: An In vitro study. J. Nanomed. Nanotechnol., 4: 1-4.

Shihabudeen, H.M.S., D.H. Priscilla and K. Thirumurugan, 2010. Antimicrobial activity and phytochemical analysis of selected Indian folk medicinal plants. Intl. J. Pharma. Sci. Res., 1: 430-434.

Smitha, S.L., K.M. Nissamudeen, D. Philip and K.G. Gopchandran, 2008. Studies on surface plasmon resonance and photoluminescence of silver nanoparticles. Spectrochim. Acta Part A. Mol. Biomol. Spectrosc., 71: 186-190.

Valadez-Vega, C., G. Alvarez-Manilla, L. Riveron-Negrete, A. Garcia-Carranca and J.A. Morales-Gonzalez *et al*., 2011. Detection of cytotoxic activity of lectin on human colon adenocarcinoma (Sw480) and epithelial cervical carcinoma (C33-A). Mols., 16: 2107-2118.

Zhang, J.H., J. Yu, W.X. Li and C.P. Cheng, 1998. Evaluation of Mn2+ stimulated and Zn2+ inhibited apoptosis in rat corpus luteal cells by flow cytometry and fluorochromes staining. Chin. J. Physiol., 41: 121-126.